Biochem. J. (2015) **465**, 239–245 (Printed in Great Britain) doi:10.1042/BJ20141120

The architecture of an Okazaki fragment-processing holoenzyme from the archaeon *Sulfolobus solfataricus*

Giuseppe Cannone*, Yuli Xu†, Thomas R. Beattie‡[1], Stephen D. Bell†‡[2] and Laura Spagnolo*[2]

*Institute of Structural and Molecular Biology, and Centre for Science at Extreme Conditions, University of Edinburgh, Edinburgh EH9 3JR, U.K.
†Molecular and Cellular Biochemistry Department, Biology Department, Indiana University, Bloomington, IN 47405, U.S.A.
‡Sir William Dunn School of Pathology, Oxford University, Oxford OX1 3RE, U.K.

DNA replication on the lagging strand occurs via the synthesis and maturation of Okazaki fragments. In archaea and eukaryotes, the enzymatic activities required for this process are supplied by a replicative DNA polymerase, Flap endonuclease 1 (Fen1) and DNA ligase 1 (Lig1). These factors interact with the sliding clamp PCNA (proliferating cell nuclear antigen) providing a potential means of co-ordinating their sequential actions within a higher order assembly. In hyperthermophilic archaea of the *Sulfolobus* genus, PCNA is a defined heterotrimeric assembly and each subunit interacts preferentially with specific client proteins. We have exploited this inherent asymmetry to assemble a PCNA–polymerase–Fen1–ligase complex on DNA and have visualized it by electron microscopy. Our studies reveal the structural basis of co-occupancy of a single PCNA ring by the three distinct client proteins.

Key words: DNA replication, Okazaki fragment maturation, proliferating cell nuclear antigen (PCNA), single particle electron microscopy.

INTRODUCTION

DNA replication requires the co-ordination of a multitude of proteins to create error-free daughter DNA strands. The two daughter strands are synthesized with different mechanisms. On the lagging strand, short RNA-primed Okazaki fragments are synthesized. RNA primers are then removed and replaced with DNA. The resulting DNA fragments are finally ligated to ensure strand continuity. *Sulfolobus solfataricus* has a simplified toolset for DNA replication compared with eukaryotes and is therefore a useful model system for the study of replication proteins [1]. In particular, *S. solfataricus* encodes a subset of the eukaryotic Okazaki fragment maturation factors, among which are the proliferating cell nuclear antigen (PCNA), as well as DNA polymerase B1, the flap endonuclease, Fen1 (Flap endonuclease 1) and an ATP-dependent DNA ligase, Lig1 (ligase 1). These proteins are necessary and sufficient for concerted DNA synthesis, RNA primer removal and strand ligation *in vitro* [2]. In *S. solfataricus*, PCNA is a heterotrimeric assembly where each subunit interacts preferentially with specific client proteins [1]. In the context of Okazaki fragment maturation, *S. solfataricus* (Sso) PCNA1 specifically interacts with Fen1, SsoPCNA2 with the replicative DNA polymerase B1 (PolB1) and SsoPCNA3 with Lig1. It is unclear how PCNA effects hand-off of DNA from polymerase and Fen1 to DNA ligase, thereby co-ordinating Okazaki fragments maturation. Biochemical studies have put forward a molecular tool-belt model, although this remains controversial [3–5]. However, recent biochemical studies [2] support a model where a single PCNA ring assembles an Okazaki fragment maturation complex composed of PolB1, Fen1 and Lig1. To address the structural basis of co-ordination of polymerase, flap nuclease and ligase activities, we assembled the PCNA–PolB1–Fen1–Lig complex on DNA and visualized it by electron microscopy (EM). Our study reveals that SsoPCNA simultaneously co-ordinates the three client proteins and, thus, facilitates co-ordination of functions in time and space in a molecular tool-belt.

MATERIALS AND METHODS

Protein purification

His-SsoPCNA1/2/3, His-SsoPolB1, SsoFen1 and SsoLig1 expression constructs were generated previously [1,6]. All proteins were over-expressed in *Escherichia coli* Rosetta (DE3) pLysS (Novagen). Cells were grown to $D_{600} = 0.4$–0.6 before induction with 1 mM IPTG for 3 h at 37 °C. Cells were harvested by centrifugation at 3980 ***g*** for 15 min. Cells expressing His-SsoPCNA1/2/3 were resuspended in 20 mM HEPES, pH 8.0, 300 mM NaCl and protease inhibitors. Extract was lysed by sonication before centrifugation at 20 100 ***g*** for 30 min. Supernatant was heated to 75 °C for 25 min before further centrifugation. The supernatant was purified by passage through 1 ml HisTrap columns (GE Healthcare) and eluted fractions were loaded on to a Superose 10/300 gel-filtration column pre-equilibrated in 20 mM HEPES, pH 8.0, and 300 mM NaCl. Protein-containing fractions were pooled and stored at − 80 °C. Cells expressing SsoPolB1 were resuspended in 10 mM HEPES, pH 7.5, 100 mM NaCl, 1 mM DTT with protease inhibitors, lysed by sonication and centrifuged at 20 100 ***g*** for 30 min. The supernatant was incubated for 20 min at 65 °C before further centrifugation. The supernatant was loaded on to a HiTrap heparin column pre-equilibrated in buffer 10 mM HEPES, pH 7.5,

Abbreviations: FAM, 6-carboxyfluorescein; Fen1, Flap endonuclease 1; FSC, Fourier Shell Correlation; hFen1, human Fen1; Lig1, ligase 1; IDCL, interdomain connector loop; PCNA, proliferative cell nuclear antigen; PIP, PCNA-interacting peptide; PolB1, polymerase B1; Sso, *Sulfolobus solfataricus*; TBE, Tris/borate/EDTA.

[1] Present address: Department of Biology, McGill University, Montreal, Quebec, Canada H3G 0B1
[2] Correspondence may be addressed to either of these authors (email laura.spagnolo@ed.ac.uk or email stedbell@imap.iu.edu).

100 mM NaCl and 1 mM DTT, and eluted over a 75-ml linear gradient of 100–1000 mM NaCl. Protein-containing fractions were loaded on to a Superose 10/300 gel-filtration column pre-equilibrated in 10 mM HEPES, pH 7.5, 500 mM NaCl and 1 mM DTT. Protein-containing fractions were diluted 5-fold in 10 mM HEPES and pH 7.5, 1 mM DTT, loaded on to a HiTrap S column (GE Healthcare) pre-equilibrated in buffer 10 mM HEPES, pH 7.5, 100 mM NaCl and 1 mM DTT, and eluted over a 30-ml linear gradient of 100–1000 mM NaCl. Protein-containing fractions were pooled and stored at − 80 °C. Cells expressing His-SsoLig1 were ground in liquid nitrogen, resuspended in 20 mM HEPES, pH 7.5, and 300 mM NaCl with protease inhibitors and incubated for 25 min at 75 °C before centrifugation at 20 100 ***g*** for 30 min. The supernatant was loaded on to a 1 ml HisTrap column (GE Healthcare) and eluted with 500 mM imidazole. Eluted fractions were loaded on a Superose 10/300 gel filtration column (GE Healthcare) pre-equilibrated in 10 mM HEPES, pH 8.0, 150 mM NaCl and 14 mM 2-mercaptoethanol. Protein-containing fractions were diluted 2-fold in 10 mM HEPES pH 8.0 14 mM 2-mercaptoethanol, loaded on to a HiTrap Q column (GE Healthcare) pre-equilibrated in 10 mM HEPES, pH 8.0, 75 mM NaCl and 14 mM 2-mercaptoethanol, and eluted over a 30-ml linear gradient of 75–1000 mM NaCl. Protein-containing fractions were pooled and stored at − 80°C SsoFen1 was purified as described previously [7]. Extracts were lysed by sonication, clarified by centrifugation before incubation for 15 min at 75 °C and further centrifugation. The supernatant was purified by passage through a HiTrap Heparin column (GE Healthcare) and a Superose gel-filtration column (GE Healthcare). Protein-containing fractions were pooled and stored at − 80 °C.

DNA oligonucleotides

DNA oligonucleotides were purchased from Sigma-Genosys. The sequences were the following (mismatch shown in bold and flap underlined): upstream: 5′-CAGGTGGGCTG-CGGTCACGTTGACTAGGGTC**G**-3′; downstream: 5′-CAAGCAGTCCTAACTTTGAGGCAGAGTCCCCCACCTAA-CTTTAA-3′; template: 5′-TTAAAGTTAGGTGGGGGACTC-TGCCTCAAGACGGTAGTCAACGTGACCGCAGCAAACC-TG-3′.

Purification of PCNA–PolB1–Lig1–Fen1–DNA complex on GraFix gradients

DNA mimicking two adjacent Okazaki fragments was prepared at a final concentration of 30 μM in a total volume of 10 μl. Oligonucleotides were mixed together and incubated in a thermocycler for 80 min at a temperature decreasing from 95 °C to 20 °C. SsoPCNA1/2/3 (1.4 μM) was pre-incubated with 1.7 μM annealed DNA in 10 mM HEPES, pH 8.0, 150 mM NaCl and 5 mM $MgCl_2$ at 50 °C for 50 min in a reaction volume of 175 μl. Following this pre-incubation, SsoPolB1, SsoLig1 and SsoFen1 were added into the reaction mix to a final concentration of 1.25 μM in a reaction volume of 200 μl and incubated for a further 30 min at 50 °C. The protein–DNA complex was then purified according to the GraFix protocol [8] using a 0–30 % glycerol gradient combined with a 0.25–0.8 % glutaraldehyde gradient, in buffer containing 10 mM HEPES, pH 8.0, 150 mM NaCl and 5 mM $MgCl_2$.

Western blots

Fractions collected from GraFix were separated on a 4–12 % Bis-Tris precast gradient gel (NuPage, Invitrogen), transferred to a nitrocellulose membrane and probed with polyclonal antibodies anti-PCNA, anti-PolB1, anti-Lig1 and anti-FEN1. Rabbit polyclonal antibodies were described by Beattie and Bell [2].

Electron microscopy

PCNA–PolB1–Fen1–Lig1 bound to DNA was studied by negative staining EM and single particle analysis. Data were collected on a FEI F20 FEG microscope, equipped with an 8k×8k CCD (charged-couple device) camera. Images were collected under low dose mode at a magnification of 50000×, at a final sampling of 1.6 Å/pixel (0.16 nm/pixel) at the specimen level. Single particle images were selected interactively using the Boxer program from the EMAN single particle analysis package [9] and extracted into boxes. Image processing was performed using the IMAGIC-5 package [10] and EMAN [9]. The dataset was re-sampled at 3.2 Å/pixel. A total of 8206 images were band-pass filtered with a high pass cut-off of 200 Å and a low pass cut-off of 1 Å. The single particle images were analysed by Multivariate Statistical Analysis with IMAGIC-5 [10]. The dataset was subjected to successive rounds of alignment and classification in order to improve the resulting image class-averages. Selected PCNA–PolB1–Fen1–Lig1–DNA class-averages were used to calculate a starting 3D volume by common lines using the Euler program in IMAGIC-5. The PCNA–PolB1–Fen1–Lig1–DNA structure was refined by projection matching using the Refine program in EMAN until the map converged. The number of particles used in the final reconstruction was 5672. The resolution of the map was calculated as 22 Å by FSC (Fourier Shell Correlation) (0.5). Figures were prepared with Chimera [11]. The PCNA–PolB1–Fen1–DNA structure was solved using the EMD-5220 map [12] as a starting model and refined with EMAN using 6878 images sampled at 6.4 Å/pixel to a resolution of ∼30 Å.

Activity assays

Flap cleavage assays were assembled with the indicated proteins and DNA, all components at 1.5 μM in a 20 μl reaction volume containing 10 mM HEPES, pH 8.0, 150 mM NaCl and 5 mM $MgCl_2$. The DNA oligonucleotides were the same as those used in GraFix with the exception that the downstream primer had a 3′ FAM (6-carboxyfluorescein) fluorophore attached. As with the GraFix procedure, DNA was pre-incubated with PCNA for 50 min at 50 °C, prior to addition of Fen1 and incubation for a further 30 min at 50 °C. Reactions were terminated by addition of 20 μl of 95 % formamide containing 20 mM EDTA, pH 8.0, and 0.005 % Bromophenol Blue. Samples were boiled for 5 min then rapidly chilled on ice prior to loading on a 12 % denaturing polyacrylamide sequencing gel [19:1 acrylamide/bisacrylamide in 1 × TBE (Tris/borate/EDTA)]. DNA was visualized by detection of the FAM fluorophore using a Typhoon 9210 (GE Healthcare) imaging system.

DNA ligase reaction mixtures (20 μl) contained 50 mM Tris/HCl pH 7.5, 10 mM $MgCl_2$, 10 mM DTT, 1 mM ATP, 100 μg/ml BSA, 50 nM DNA substrates, 125 nM ligase and indicated amounts of PCNA (12 nM, 1.2 nM, 120 pM) and were incubated for 30 min at 55 °C. Reactions were terminated by addition of 20 μl of loading dye (8 M urea, 1 × TBE and 0.05 % Bromophenol Blue). Samples were boiled for 5 min at 100 °C. Reaction products were resolved by electrophoresis through a 12 % polyacrylamide, 8 M urea, 1 × TBE gel. DNA was visualized by detection of the CY5 fluorophore using a Typhoon 9210 (GE Healthcare) imaging system.

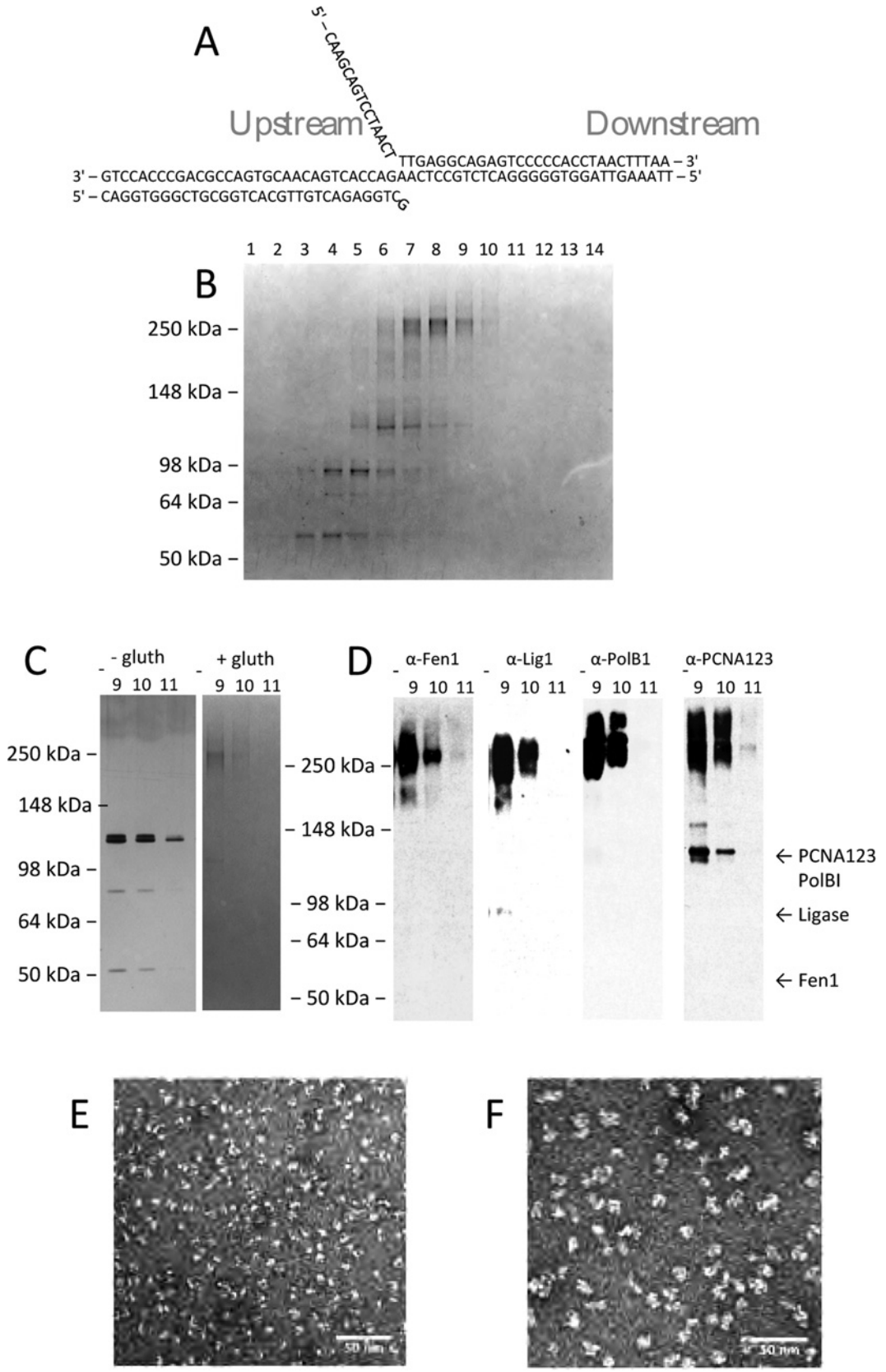

Figure 1 Purification of the PCNA–PolB1–Fen1–Lig1–DNA complex of *S. solfataricus*

(**A**) DNA structure used in the GraFix input. (**B**) SDS/PAGE analysis of fractions from a GraFix gradient. (**C**) Comparison between control fractions from gradients run without cross-linker and GraFix fractions gluth, glutaraldehyde. (**D**) The presence of all four proteins in the cross-linked samples was assessed by Western blotting. (**E**) Sample screening: the complex fractionated from pycnic gradients not containing glutaraldehyde disassembles upon EM sample preparation. (**F**) Sample screening: samples collected from GraFix gradients are stable during negative staining sample preparation.

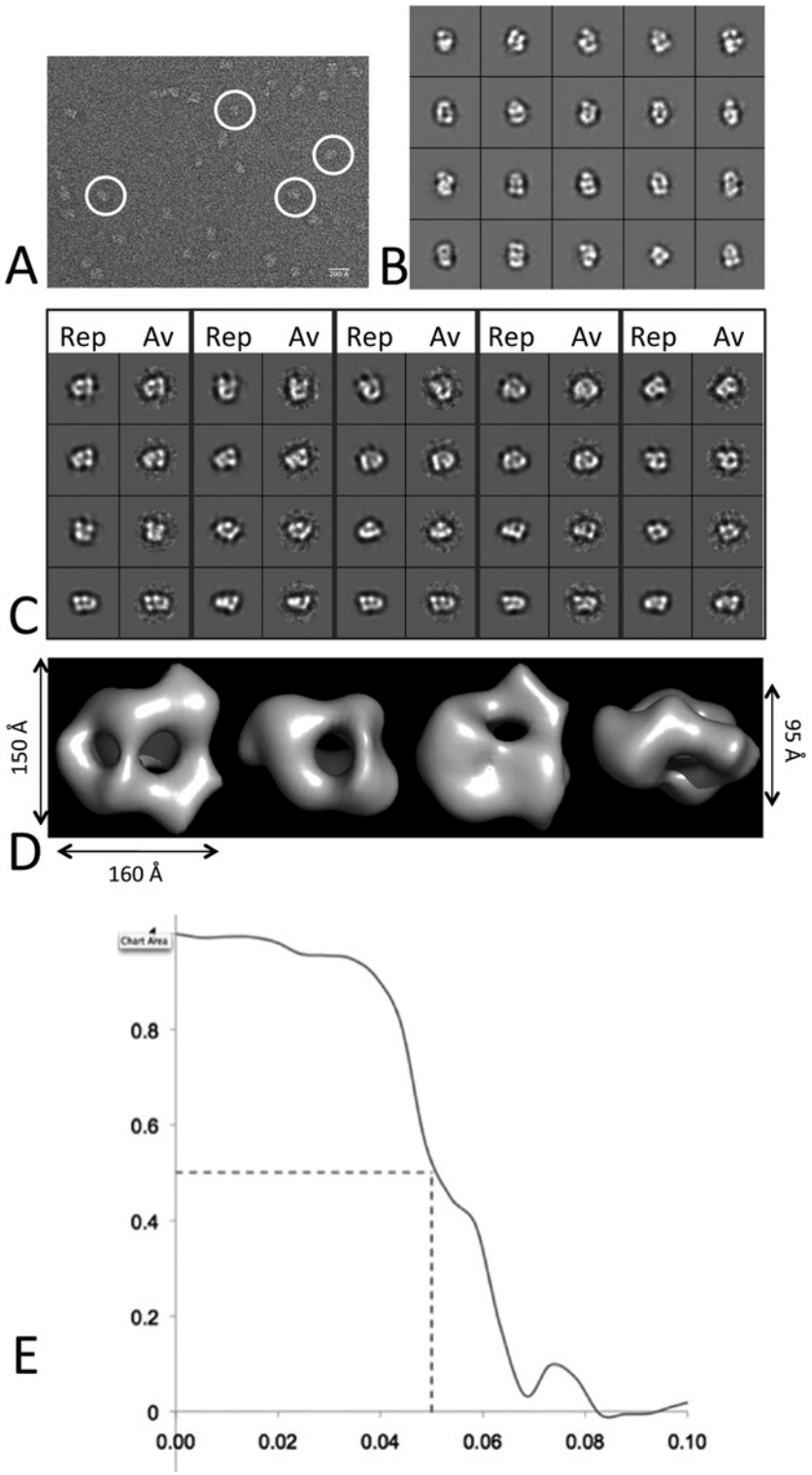

Figure 2 3D-EM visualization of the PCNA–PolB1–Fen1–Lig1–DNA complex

(**A**) Characteristic negatively-stained micrograph. White circles are used to show single particles. (**B**) Reference-free class averages calculated with Imagic-5 show a three-layered architecture. Box size: 410 Å. (**C**) Reprojections and class averages for the refined 3D reconstruction. Box size: 410 Å. (**D**) 3D model of the PCNA–PolB1–Fen1–Lig1–DNA complex. (**E**) FSC plot with 0.5 point highlighted.

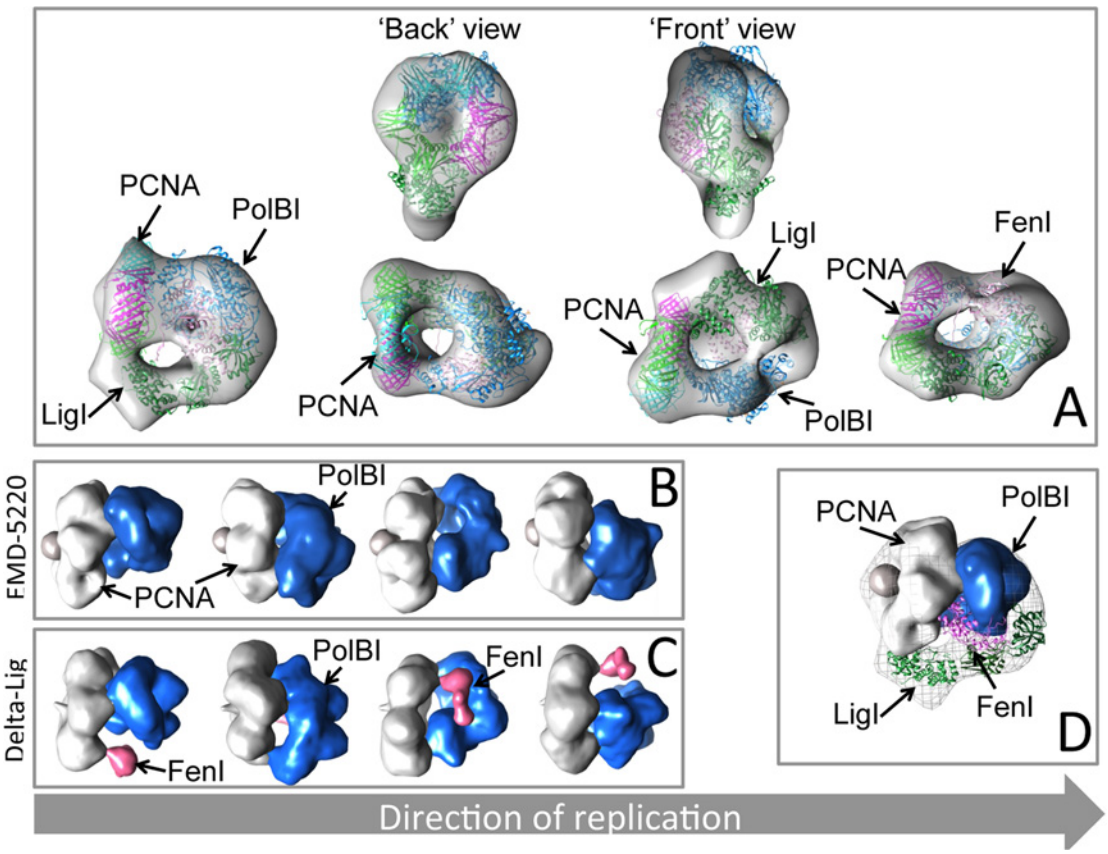

Figure 3 Fitting the protein components within the PCNA–PolB1–Fen1–Lig1–DNA complex

(**A**) Back and front views of the 'Okazakisome' 3D-EM model. The volumes and shapes of 1UL1, 2HIV and 1SJ5 fitted in the Okazakisome map are consistent with a PCNA ring on which Fen1, LigI and PolBI are simultaneously bound on one face of PCNA. (**B** and **C**) Structural comparison of EMD-5220 and PCNA–Pol–Fen1 on DNA. EMD-5220: PCNA is shown in grey, DNA in darker grey, Pol is shown in blue. PCNA–Pol–Fen1 on DNA. PCNA is coloured grey, Pol is coloured blue, Fen1 is coloured pink. (**D**) EMD-5220 (PCNA and DNA in grey, Pol in blue), 1UL1 chain Y (pink) and 2HIV in extended conformation (green) fitted in the Okazakisome map.

Substrate 1 was prepared by annealing the following oligonucleotides 5′ Cy5-GATCGTGGCTATTGTCGCCCTTAT-TCCGAC and 5′ phosphate-AGTGACACATTTTTGTGTCAC-TGTCGGAATAAGGGCGACAATAGCCACGATC and substrate 2 used annealed 5′ Cy5-GATCGTGGCTATTGTCGCC-CTTATTCCGACAGTGACACATTTTTGTGTCACT 3′ and 5′ phosphate-GTCGGAATAAGGGCGACAATAGCCACGATC 3′.

RESULTS AND DISCUSSION

We reconstituted the PCNA–PolB1–Fen1–Lig complex from recombinant proteins loaded on a 60 bp dsDNA template featuring a mismatch and a flap (Figure 1) and analysed it by EM coupled to single particle analysis (Figures 2 and 3). The DNA was designed based on a crystallographic paper on human Fen1 (hFen1) in complex with DNA [13] and shown to be cleaved by Fen1 (Figure 4). The 'Okazakisome' was assembled from individually purified components, including a fully functional PCNA molecule in which the three subunits are expressed as a covalently-linked concatamer [2,6], which were loaded on GraFix gradients [8]. Gradients devoid of cross-linker were run as controls. Fractions were analysed by SDS/PAGE and Western blotting (Figures 1B–1D) and those containing all four proteins were analysed by EM (Figure 2). It should be noted that the presence of cross-linker can alter the electrophoretic mobility of cross-linked complexes, resulting in smeared bands. The presence of all four proteins in these fractions was confirmed by MS (not shown). While the four protein species migrate to the same glycerol concentration in non-cross-linked as well as GraFix gradients (Figure 1C), the complex purified in the absence of glutaraldehyde disassembles upon preparation for EM analysis (Figures 1E and 1F), most probably on dilution.

Reference-free 2D single particle analysis highlighted a bell-shaped assembly (Figure 2B). Subsequent 3D analysis allowed the reconstruction of a bell-shaped complex (Figure 2C). The volume of this 3D reconstruction (Figure 2D) is compatible with a molecular weight of 350 kDa, the predicted mass for the full complex of proteins with DNA. The overall dimensions of the complex are 160 × 150 × 95 Å (Figure 2D). FSC analysis using the 0.5 criterion gives a resolution of ∼22 Å, compatible with the level of detail exhibited by the 3D map. We have determined that Fen1 is active under the conditions of complex preparation, resulting in flap cleavage (Figure 4A).

To interpret our 3D-EM reconstruction, we used the structures calculated for its isolated components and for the three sub-complexes PCNA–Fen1, PCNA–PolI–DNA and PCNA–Lig1–DNA. This fitting could lead to two different Okazakisome architectures: one with PCNA layered between its client proteins and the other one with PCNA carrying the three client proteins at the front face. Sliding clamps have unique front and back faces. Although a previous study showed that ubiquitin interacts with

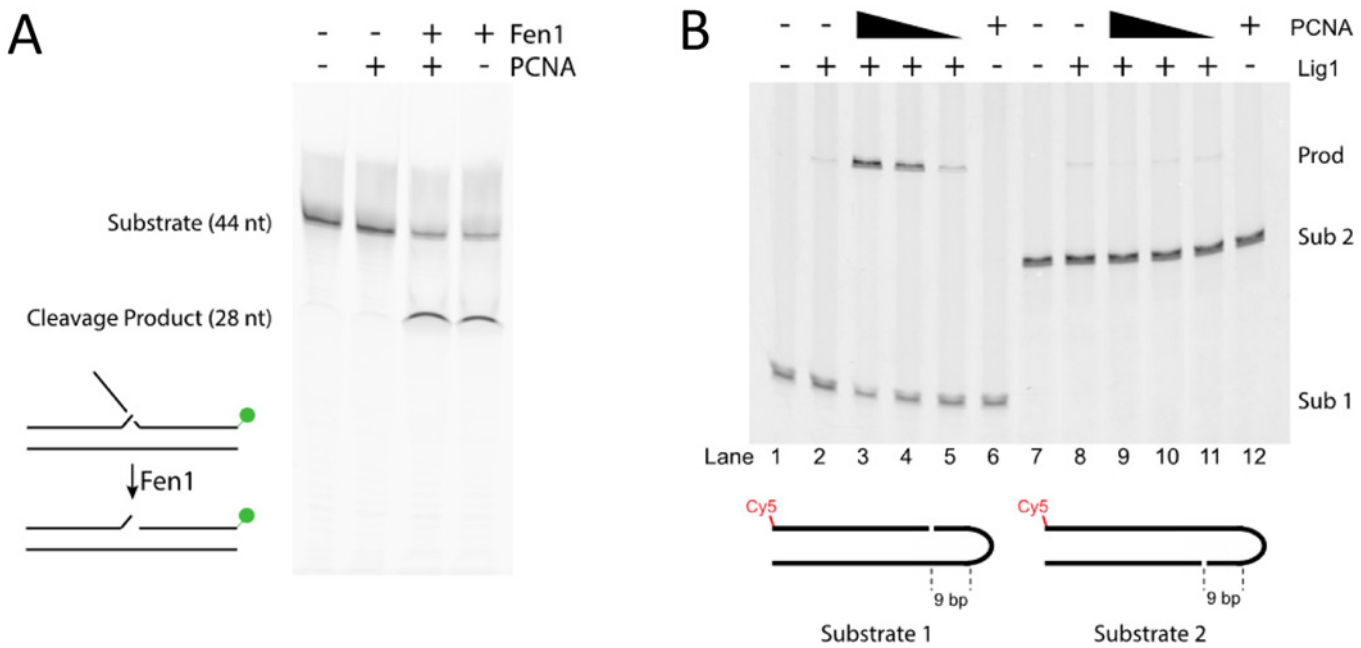

Figure 4 Activity assays

(**A**) Flap cleavage assay: reaction mixtures contained the indicated proteins at 1.5 μM. Following termination of the cleavage reaction, samples were denatured and electrophoresed on a 12% denaturing polyacrylamide gel. The positions of migration of the substrate and cleavage product are indicated. The schematic diagram to the left of the gel indicates the substrate and product with the FAM fluorophore represented by a green circle. (**B**) Ligation assays: reaction mixtures contained the indicated nicked hairpin DNA substrates. Relative migration of substrates (Sub1 and Sub2) and ligation products (Prod) are indicated to the right of the gel image. Lanes 1 and 7 lacked protein. Lanes 2–5 and 8-11 contained 125 nM DNA Lig1. Lanes 3 and 9, 4 and 10 and 5 and 11 had 12 nM, 1.2 nM and 0.12 nM PCNA added respectively.

the back face of PCNA [14], it is generally believed that client proteins interact with the front face of PCNA. Indeed, the principal contact point on PCNA for client proteins, the IDCL (interdomain connector loop), is found towards the front face of the PCNA ring. Notably, the IDCL-interacting motif within the ligase, which is required for functional interaction with PCNA, is found within a short internal loop in the ligase [19]. Spatial constraints suggest it is unlikely that Lig1 could dock with the IDCL of PCNA yet be located behind the ring. Nevertheless, to discriminate between the two possible map interpretations, we performed an activity assay in which we tested the preference of the ligase for either a front-face or a back-face interaction. We designed two hairpin DNA substrates of the same overall sequence composition but with nicks on opposite strands. The positioning of the nick 9 base pairs from the hairpin limits the length of DNA available for interaction with Lig1 and PCNA. If PCNA functionally interacts with Lig1 via PCNA's front-face, then substrate 1 should reveal PCNA-stimulated ligation; if interaction with the back-face of PCNA stimulates ligase then substrate 2 would show PCNA-enhancement of ligase activity. As seen in Figure 4(B), basal ligase activity on both substrates is equivalent, however, only substrate 1 shows PCNA-dependent stimulation of Lig1 activity. Thus, our functional data support the fitting of all three client proteins on the front face of the PCNA ring.

Additionally, we performed the GraFix procedure with DNA, PolB1, Fen1 and PCNA in the absence of Lig1. The resultant particles lack the density ascribed to Lig1 in the full Okazakisome (Figures 3; Supplementary Figure S1).

The fully assembled Okazakisome (Figures 2 and 3) exhibits features compatible with previous EM studies of related sub-assemblies (PCNA–Lig–DNA [5] and PCNA–Pol–DNA [12]). To glean insight into the mechanism by which PCNA co-ordinates three client proteins to process Okazaki fragments, we fitted each constituent of the assembly using Chimera, based on their volumes and shapes (Figure 3).

It is not possible to determine unambiguously the trajectory of DNA within the complex. This could be because the DNA we designed to load one and only one copy of PCNA is completely embedded in the structure. We used crystallographic structures for the SsoPCNA ring (2NTI [15]), for the hPCNA–Fen1 complex (1UL1 [16]) and for the SsoPCNA1/2 in complex with Fen1 (2IZO [17]) to define the position of the sliding clamp within the map. 1UL1 and 2IZO facilitated docking and map interpretation since they have distinct asymmetric shapes. In 1UL1, each Fen1 molecule (chains X, Y and Z in the PDB file) crystallized in a distinct conformation [16]. We tested fitting assemblies ABCX, ABCY and ABCZ from 1UL1. Based on the ligation experiment, we placed the PCNA ring at one end of the EM model, which exhibits a round shape. The complex is assembled on DNA, therefore the central cavity of PCNA is filled. The Fen1 Y-chain from 1UL1 was the one that could better be accommodated in the EM density for Fen1 (Figure 3). This is analogous to what was shown in the crystallographic study of the SsoPCNA1/'2 dimer associated to Fen1 [17], where the conformation of the endonuclease recalls the Y-chain in 1UL1. We used the EM reconstructions for PCNA–LigI–DNA and PCNA–PolBI–DNA (maps EMDB-5220 and EMDB-1485 [5,12]) as probes to assign densities for PCNA-containing subcomplexes. To fit individual client proteins, we used the PDB codes: 1UL1 [16] and 2IZO [17] for the PCNA–Fen1 complex (Figure 3B), 1S5J [18] for PolB (Figure 3C) and 2HIV [19] for the ligase.

Combining the analysis of the map with the biochemical information available on the PCNA interaction with the client proteins [1,2], we modelled PCNA2 interacting with the PCNA-interacting peptide (PIP) box of PolB1 and PCNA3 with the PIP box in Lig1. 1S5J fits extremely well in the density connecting

PCNA2 and PCNA3 (Figure 3), forming two extensive contacts with the PCNA ring, consistent with the EM analysis of the PCNA–polymerase complex loaded on DNA [12].

We fitted the ligase at the front face of the PCNA ring in our EM map using the crystallographic data for the full-length *Sulfolobus* protein (2HIV [19]) and of hLigase$_{233–919}$ in complex with DNA (1X9 N [20]). A variety of studies have revealed that ligase1 is a very flexible molecule [19]. We performed its fitting placing the PIP-box containing nucleotide close to PCNA3, in the extended conformation of 2HIV, the crystal structure for the DNA-free ligase [19]. The model shown in Figure 3 is in very good agreement with the 3D superposition of PCNA–Pol, PCNA–Fen1 and PCNA–Lig1 (1UL1, EMDB-5220 and EMDB-1485). The main difference is the extended conformation of the ligase. The conformational malleability of Lig1 is highlighted by crystallographic structures which have revealed that ligase fully encircles the nicked-DNA substrate to effect ligation. We speculate that when ligase adopts this final conformation, it may displace DNA polymerase and Fen1, allowing their recycling to the next Okazaki fragment.

To further confirm the fitting of the ligase within the Okazakisome, we assembled a partial complex composed of PCNA–Pol–Fen1 on DNA. We determined its 3D structure using the EMD-5220 map as a starting model (Supplementary Figure S1). We compared the PCNA–Pol starting model (Figure 3B) with our PCNA–Pol–Fen1 assembly (Figure 3C) and clearly saw a density (coloured pink in Figure 3C) compatible with the speculated position of Fen1 within the PCNA ring. Fitting EMD-5220, 1UL1 (chain Y) and 2HIV in the Okazakisome (Figure 3D) is compatible with Lig1 in an extended conformation on the front face of the assembly.

Conclusions

According to our structure, PCNA can load one client protein per subunit, forming a stable complex on DNA. The positioning of ligase in its extended conformation prevents steric clashes with the other client proteins. Our work reveals the answer to a long-debated biological question, showing that PCNA can orchestrate the action of client proteins according to the 'tool-belt model', instead of loading just one client protein at one given time.

AUTHOR CONTRIBUTION

Laura Spagnolo and Stephen D. Bell conceived the work. Giuseppe Cannone, Yuli Xu, Stephen D. Bell and Laura Spagnolo performed the experiments. Thomas R. Beattie provided antibodies and protocols. Laura Spagnolo and Stephen D. Bell wrote the manuscript.

FUNDING

This work was supported by the Darwin Trust of Edinburgh studentship (to G.C.); the Biotechnology and Biological Sciences Research Council (to T.R.B.); the Wellcome Trust Programme [grant number 086045/Z/08/Z] and the College of Arts and Sciences, Indiana (to S.D.B.); The Royal Society [grant number R41318]; the Cancer Research U.K. [grant number C17335/A10470]; the Biotechnology and Biological Sciences Research Council [grant number BB/J005673/1] to L.S.; and the EM Facility at Edinburgh is supported by the Scottish Alliance for Life Sciences and the Wellcome Trust [grant number WT087658MA].

Received 3 September 2014/7 October 2014; accepted 9 October 2014
Published as BJ Immediate Publication 9 October 2014, doi:10.1042/BJ20141120

REFERENCES

1 Dionne, I., Nookala, R. K., Jackson, S. P., Doherty, A. J. and Bell, S. D. (2003) A heterotrimeric PCNA in the hyperthermophilic archaeon *Sulfolobus solfataricus*. Mol. Cell. **11**, 275–282 CrossRef PubMed
2 Beattie, T. R. and Bell, S. D. (2012) Coordination of multiple enzyme activities by a single PCNA in archaeal Okazaki fragment maturation. EMBO J. **31**, 1556–1567 CrossRef PubMed
3 Subramanian, J., Vijayakumar, S., Tomkinson, A. E. and Arnheim, N. (2005) Genetic instability induced by overexpression of DNA ligase I in budding yeast. Genetics **171**, 427–441 CrossRef PubMed
4 Levin, D. S., McKenna, A. E., Motycka, T. A., Matsumoto, Y. and Tomkinson, A. E. (2000) Interaction between PCNA and DNA ligase I is critical for joining of Okazaki fragments and long-patch base-excision repair. Curr. Biol. **10**, 919–922 CrossRef PubMed
5 Mayanagi, K., Kiyonari, S., Saito, M., Shirai, T., Ishino, Y. and Morikawa, K. (2009) Mechanism of replication machinery assembly as revealed by the DNA ligase-PCNA-DNA complex architecture. Proc. Natl. Acad. Sci. U.S.A. **106**, 4647–4652 CrossRef PubMed
6 Dionne, I., Brown, N. J., Woodgate, R. and Bell, S. D. (2008) On the mechanism of loading the PCNA sliding clamp by RFC. Mol. Microbiol. **68**, 216–222 CrossRef PubMed
7 Hutton, R. D., Roberts, J. A., Penedo, J. C. and White, M. F. (2008) PCNA stimulates catalysis by structure-specific nucleases using two distinct mechanisms: substrate targeting and catalytic step. Nucleic Acids Res. **36**, 6720–6727 CrossRef PubMed
8 Stark, H. (2010) GraFix: stabilization of fragile macromolecular complexes for single particle cryo-EM. Methods Enzymol. **481**, 109–126 CrossRef PubMed
9 Ludtke, S. J., Baldwin, P. R. and Chiu, W. (1999) EMAN: semiautomated software for high-resolution single-particle reconstructions. J. Struct. Biol. **128**, 82–97 CrossRef PubMed
10 van Heel, M., Harauz, G., Orlova, E. V., Schmidt, R. and Schatz, M. (1996) A new generation of the IMAGIC image processing system. J. Struct. Biol. **116**, 17–24 CrossRef PubMed
11 Goddard, T. D., Huang, C. C. and Ferrin, T. E. (2007) Visualizing density maps with UCSF Chimera. J. Struct. Biol. **157**, 281–287 CrossRef PubMed
12 Mayanagi, K., Kiyonari, S., Nishida, H., Saito, M., Kohda, D., Ishino, Y., Shirai, T. and Morikawa, K. (2011) Architecture of the DNA polymerase B-proliferating cell nuclear antigen (PCNA)-DNA ternary complex. Proc. Natl. Acad. Sci. U.S.A. **108**, 1845–1849 CrossRef PubMed
13 Tsutakawa, S. E., Van Wynsberghe, A. W., Freudenthal, B. D., Weinacht, C. P., Gakhar, L., Washington, M. T., Zhuang, Z., Tainer, J. A. and Ivanov, I. (2011) Solution X-ray scattering combined with computational modeling reveals multiple conformations of covalently bound ubiquitin on PCNA. Proc. Natl. Acad. Sci. U.S.A. **108**, 17672–17677 CrossRef PubMed
14 Freudenthal, B. D., Gakhar, L., Ramaswamy, S. and Washington, M. T. (2010) Structure of monoubiquitinated PCNA and implications for translesion synthesis and DNA polymerase exchange. Nat. Struct. Mol. Biol. **17**, 479–484 CrossRef PubMed
15 Hlinkova, V., Xing, G., Bauer, J., Shin, Y. J., Dionne, I., Rajashankar, K. R., Bell, S. D. and Ling, H. (2008) Structures of monomeric, dimeric and trimeric PCNA: PCNA-ring assembly and opening. Acta Crystallogr. D. Biol. Crystallogr. **64**, 941–949 CrossRef PubMed
16 Sakurai, S., Kitano, K., Yamaguchi, H., Hamada, K., Okada, K., Fukuda, K., Uchida, M., Ohtsuka, E., Morioka, H. and Hakoshima, T. (2005) Structural basis for recruitment of human flap endonuclease 1 to PCNA. EMBO J. **24**, 683–693 CrossRef PubMed
17 Dore, A. S., Kilkenny, M. L., Jones, S. A., Oliver, A. W., Roe, S. M., Bell, S. D. and Pearl, L. H. (2006) Structure of an archaeal PCNA1-PCNA2-FEN1 complex: elucidating PCNA subunit and client enzyme specificity. Nucleic Acids Res. **34**, 4515–4526 CrossRef PubMed
18 Savino, C., Federici, L., Johnson, K. A., Vallone, B., Nastopoulos, V., Rossi, M., Pisani, F. M. and Tsernoglou, D. (2004) Insights into DNA replication: the crystal structure of DNA polymerase B1 from the archaeon *Sulfolobus solfataricus*. Structure **12**, 2001–2008 CrossRef PubMed
19 Pascal, J. M., Tsodikov, O. V., Hura, G. L., Song, W., Cotner, E. A., Classen, S., Tomkinson, A. E., Tainer, J. A. and Ellenberger, T. (2006) A flexible interface between DNA ligase and PCNA supports conformational switching and efficient ligation of DNA. Mol. Cell. **24**, 279–291 CrossRef PubMed
20 Pascal, J. M., O'Brien, P. J., Tomkinson, A. E. and Ellenberger, T. (2004) Human DNA ligase I completely encircles and partially unwinds nicked DNA. Nature **432**, 473–478 CrossRef PubMed